HAL open science

Influence of the thermally induced deflection of a space micro-concentrator photovoltaic array on its optical performances using finite element method

Victor Vareilles, Anderson Bermudez Garcia, Fabien Chabuel, Mohamed Amara, Yannick Veschetti, Philippe Voarino

To cite this version:

Victor Vareilles, Anderson Bermudez Garcia, Fabien Chabuel, Mohamed Amara, Yannick Veschetti, et al.. Influence of the thermally induced deflection of a space micro-concentrator photovoltaic array on its optical performances using finite element method. CPV-18 - 18th International conference on Concentrator Photovoltaic Systems, Apr 2022, Miyazaki, Japan. cea-04121832

HAL Id: cea-04121832

https://cea.hal.science/cea-04121832v1

Submitted on 8 Jun 2023

HAL is a multi-disciplinary open access archive for the deposit and dissemination of scientific research documents, whether they are published or not. The documents may come from teaching and research institutions in France or abroad, or from public or private research centers.

L'archive ouverte pluridisciplinaire **HAL**, est destinée au dépôt et à la diffusion de documents scientifiques de niveau recherche, publiés ou non, émanant des établissements d'enseignement et de recherche français ou étrangers, des laboratoires publics ou privés.

Influence of the Thermally Induced Deflection of a Space Micro-Concentrator Photovoltaic Array on its Optical Performances Using Finite Element Method

Victor Vareilles[1, 2, a)], Anderson Bermudez-Garcia[1], Fabien Chabuel[1], Mohamed Amara[2], Yannick Veschetti[1], Philippe Voarino[1]

[1]*Univ. Grenoble Alpes, CEA, Liten, Campus Ines, 73375 Le Bourget du Lac, France*
[2]*Univ Lyon, CNRS, INSA Lyon, ECL, UCBL, CPE Lyon, INL, UMR5270, F-69621 Villeurbanne CEDEX, France*

[a)] Corresponding author: victor.vareilles@cea.fr

Abstract. A highly integrated micro-concentrator design for space applications with a 30X concentration factor is under study. It is composed of a mirror network embedded into a honeycomb structure, stiffened with composite sheet. The micro-cells are soldered on a thin glass mounted on top of the mirrors. Because of the huge range of temperature in space applications and the asymmetry of the micro-concentrator, temperature changes could induce structural bending, modifying the incident angle of the light and straining the components. This paper focuses on the influence of the curvature on the optical performances of the design. A parametric study coupling finite element method and ray tracing simulations was conducted to evaluate the impact of the thickness of the different layers and to design a suitable structure for space applications. Four configurations with a low curvature were identified, while keeping the space mass and volume constrains in mind. Ultimately, the maximum longitudinal dimension of a panel reaching the target of 5% optical losses was determined for each of the four configurations reaching a minimum length of about 1.7 m.

INTRODUCTION

Concentrator PhotoVoltaics (CPV) could be a solution to power satellites for GEOstationary (GEO) missions [1]. These missions needs more than 15 kW at End of Life, and solar panels made with honeycomb structure could have large areas (e.g. 4 x 5 meters). The first CPV powered mission *Deep Space 1* launched in 1998 used the SCARLET panels that were about 1.6 x 1.1 meters large [2]. Micro-Concentrator PhotoVoltaic (micro-CPV) is a space tested technology that could decrease the cost of space solar generators and answer the increasing power demand. The Pennsylvania University has recently presented a micro-concentrator design using a reflective lenslet array and 200 x 200 µm solar cells [3].

We are currently working on an innovative micro-CPV design for space applications (see Figure 1) [4]. As standard flat space photovoltaic panels are made with a honeycomb sandwich structure, our design proposes to push this structure further by embedding the optical system into an aluminium honeycomb so that the optics do not increase the volume of the structure. The use of mirror allows for lighter optics with no chromatic aberrations compared to lenses. The solar cells are soldered on a cover glass atop of the optics. This ensemble is in turn bonded on top of another sandwich structure for structural reasons. However, the layers of the structure have different Coefficients of Thermal Expansion (CTE), which will lead to the bending of the panel when the temperature changes. In particular, in the GEO orbit, temperature ranges from - 180°C to + 80°C. This thermally induced deflection would modify the angle of the incident light on the surface of the panel, leading to a degradation of the optical performances, and mechanical stress, especially in the glass. This work aims to study the influence of the geometry of the structure on its thermally induced curvature and its influence on the optical performances. For this purpose, a parametric study with design of experiments was conducted. Ray racing simulations were performed to determine the optical losses as function of the incident angle. Finite Element Method (FEM) simulations were then performed to determine the curvature of the

panels and the associated incident angle. Statistical analysis was finally used to determine the effects of the parameters of the study and the configurations with the lower optical losses.

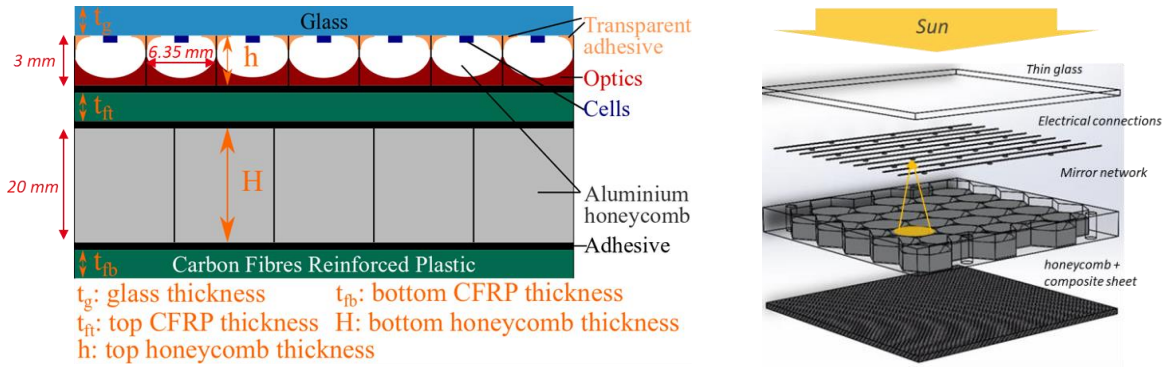

(a) (b)

FIGURE 1. Scheme (left) and exploded CAD view (right) of the concentrator design.

METHOD

Parametric study

The first step consisted in defining the variables of the parametric study. Equation 1 gives the curvature *1/R* of a bilayer strip made of two materials 1 and 2 after a temperature change ΔT. E_1 and E_2 are the respective elasticity moduli of materials 1 and 2. h_1 and h_2 are the respective thickness of the materials and γ_1 and γ_2 their Coefficient of Thermal Expansion (CTE). As space-grade materials need to be used, the elastic moduli and CTEs of the layers were fixed. The strain $(\gamma_1 - \gamma_2)\Delta T$ and thus the stress do not depend on the length of the panel. The maximum deflection does depend on the length of the panel, but the dependence can be obtained via appropriate curve fitting (see the FEM model section). Therefore, the panel length was arbitrarily set to 2000 mm.

Eventually, the chosen parameters were the thickness of the different layers (H, h, t_g, t_{ft}, t_{fb}) and are presented in Figure 1. A summary of is their levels are given in Table 1. This would give a total of 1024 configurations to test. However, thanks to the use of statistical analysis only 40 were needed to assess the effects of the parameters using the JMP software.

$$\frac{1}{R} = \frac{6E_1E_2(h_1+h_2)h_1h_2}{E_1^2h_1^4 + E_2^2h_1^4 + 4E_1E_2h_1^3h_2 + 6E_1E_2h_1^2h_2^2 + 4E_1E_2h_2^3h_1} \times (\gamma_1 - \gamma_2)\Delta T \quad (1)$$

TABLE 1. Summary of the variables and their levels

H (mm)	h (mm)	t_g (mm)	t_{ft} (mm)	t_{fb} (mm)
15	3	0.1	0.2	0.2
20	5	0.2	0.4	0.4
25	10	0.5	0.6	0.6
30	15	1	0.8	0.8

Ray Tracing model

In order to evaluate the panel curvature impact on the optical efficiency of the array, ray-tracing simulations were performed using the TracePro software based on Monte Carlo simulations. The AM0 spectrum (1366 W/m²) was used, with a spectral response from λ = 0.3 to 1.8 µm and a half solar angle of ≈ 0.27 °. A million rays were considered. Only one honeycomb cell was modelled as it is enough to study the influence of the angle of incidence. The honeycomb cells are quasi regular hexagons, the longitudinal dimension is 6.35 mm (*x-axis)* and the transverse one 4.75 mm (*y-axis)*. The origin $z = 0$ is the front side of the cell. However, as the cells are soldered on the glass, simulations were performed with cell surface positions ranging from -100 to -200 µm along the *z-axis*, to take the solder bump into account. The cells were considered as perfect absorbers and their dimensions were set to

885 x 685 µm. The glass itself was defined as a low-iron borosilicate glass with a thickness of 400 µm and no anti-reflection coating. Its refractive index $n(\lambda)$ was defined as $n(\lambda) = 1.3985 - 3.8 \times 10^{-9}\lambda^2 + 38.6 \times 10^2\lambda^{-2}$ using a fit of the Schott dispersion formula. Two electrical tracks were added, each being 100 µm wide (see Figure 2). The shading of the solar cell and the tracks was considered. The mirror is parabolic, made of a silver coating on silicone and its focal point is on the downside of the solar cell surface, assuming there is no solder bump, so in $z = 0$. This way, the focal spot covers about 40% of the cell surface when the cell is in $z = -150$ µm. Its reflective properties were taken from Kennedy *et al* [5] and DiGrazia *et al* [6]. The surface roughness of the mirror was not taken into account.

FEM model

The thermal deflection of multi-layered structures has been extensively studied [7] [8], as it is critical in several microelectronic applications. In such models, one layer is considered thicker than the other ones by several orders of magnitude, corresponding to layers of a few nanometres on a substrate in the range of a 100 µm. In our model, the thickness of the thinner and the thicker layer are 0.1 mm and 30 mm respectively. Thus, the same hypothesis cannot be made and the analytical models are not suited for this study. Instead, FEM simulations were performed with Abaqus.

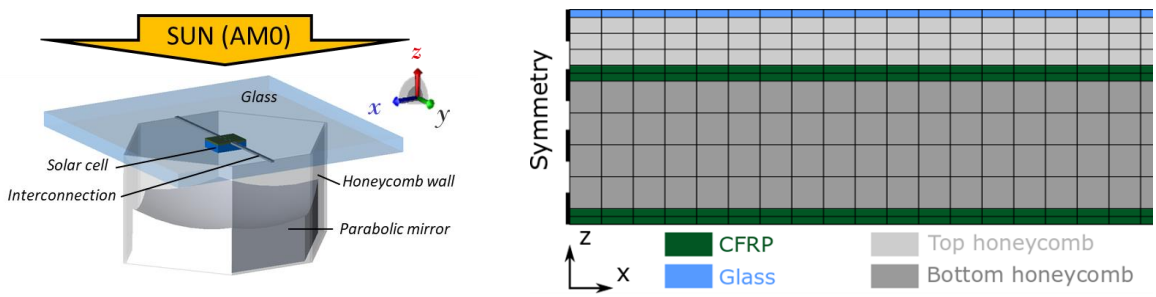

(a) (b)

FIGURE 2. Scheme of the ray tracing model (a) and of the FEM model (b).

Considering the panels as plates, quadrangles second order elements with plane strain hypothesis were used. Symmetry conditions were applied on one edge of the structure, i.e. its position was fixed. The materials were considered perfectly elastic and their mechanical and thermal properties constant over the temperature range considered. The glass and Carbon Fibres Reinforced Plastics (CFRP) were considered isotropic. The mechanical properties of the glass were taken from the space-grade CMG glass datasheet from QiOptiq. Concerning the CFRP, a plain weave cloth was assumed with M55J carbon fibres from Toray and a M18 epoxy matrix from Hexcel. The fibres volume was considered to be 60% and the elasticity modulus determined accordingly. The CTE value of the laminate was estimated from *Johnson et al* [9] and *Nawab et al* [10]. The CTE value of the honeycomb was taken from *Li et al* [11]. The elasticity and shear modulus of the honeycombs were determined in a previous study conducted at CEA-Liten. The mechanical properties of the materials can be found in Table 2.

TABLE 2. Mechanical properties used in the simulations

Materials	Bottom honeycomb	Top honeycomb	Glass	CFRP
E_x (MPa)	685	342	77×10^3	169×10^3
E_z (MPa)	1310	234	/	/
E_y (MPa)	685	342	/	/
G_{xz} (MPa)	565	186	/	/
G_{yz} (MPa)	244	99	/	/
G_{xy} (MPa)	565	186	/	/
υ	0	0	0.2	0.1
CTE (10^{-6}/K)	2	2	5.5	1.5

The temperature was assumed homogeneous in the whole assembly. In order to define the temperature difference to be applied to represent space conditions, the initial temperature must be chosen accordingly to the manufacturing process. First, the two honeycombs and the two CFRP layers are assembled in a laminator. One can assume that a flat

assembly at room temperature can be obtained at this step. Second, the glass layer is glued on the top honeycomb. The cure is usually done at room temperature, so the structure was considered flat at 298 K. The ΔT applied was - 205 K to emulate the panel temperature going from 298 to 93 K in space. A scheme of the model is shown in Figure 2.

The FEM model gives the *y* displacement as function of the position *x*, giving the final shape of the panel. Figure 3 shows an example of the deformed shape of a panel (blue curve) after a temperature decrease. Its tangent at one point is shown in orange and the normal to the panel at the same point is in black. The sunrays are symbolized by the yellow arrows. As the curvature of the panel is cylindrical, the deflection *y* at any point *x* of the panel can be fitted as $y = ax^2$. The tangent of equation ($y' = 2ax + constant$) and the unitary vector $\vec{t}(\frac{1}{\sqrt{1+4(ax)^2}}\ ;\frac{2ax}{\sqrt{1+4(ax)^2}})$ are collinear. The sunrays can be described by the unitary vector $\vec{r}(0\ ;\ 1)$. Thus, the angle α between the two vectors is described by the following equation:

$$\vec{t}.\vec{r} = \cos(\alpha) = \frac{2ax}{\sqrt{1+4(ax)^2}} \tag{2}$$

Therefore, the maximum incident angle i_{max} between the sunrays and the normal to the panel at any point of abscissa *x* is given by:

$$i_{max} = arcsin\left(\frac{2aL}{\sqrt{1+4(aL)^2}}\right) \tag{3}$$

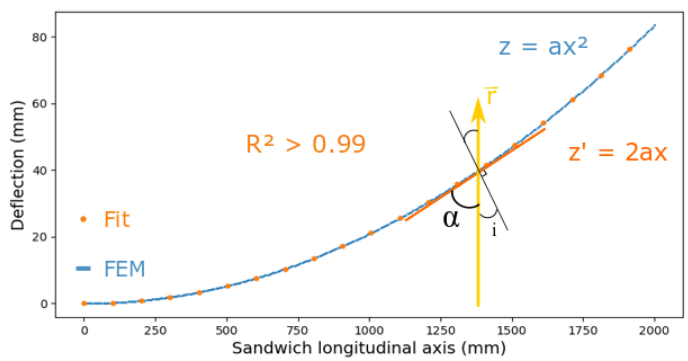

FIGURE 3. Example of a deflection curve and scheme of the problem. FEM results (line) and quadratic fit (dots).

RESULTS

Three bending cases were considered : rotation around the *x-axis*, *y-axis* and both axis at the same time. Figure 4 shows examples of irradiance maps at the angle of acceptance for the three cases and *z* = -150 µm. From this results the flux distribution is obtained. The acceptance angle, the angle at which 90% of the incident flux reaches the detector, is higher for the *y-axis* rotation case and minimum when both rotation are simultaneous. Because the *x* = 0 plane of the panel is fixed in the FEM model, one can assume that the maximum curvature of the panel will be reached around the *y-axis*, while the curvature around the *x-axis* will be significantly smaller. Thus, the *x* axis of the optics should match the *x* direction of the panel so that the highest acceptance angle is correspond to the highest curvature. The bending around the *y-axis* will therefore be considered the limiting one in terms of optical losses. Then, total flux curves as function of the incident angle were obtained, for a cell position varying between -100 and -200 µm (Figure 5). In the worst case scenario, when the cell is in *z* = -200 µm, the acceptance angle is 4.5° and optical losses as low as 5% are reached when the incident angle remains below 3°.

As explained earlier, the FEM simulations were statistically analysed to determine the influence of the layers thicknesses on the incident angle. The glass thickness has the highest impact and should be minimised to decrease the deflection. However, considering that a 100 µm thick glass could cause manufacturing issues, a thickness of 300 µm will not be discarded at this stage. The bottom honeycomb and CFRP layer both have a high impact and should be maximised. The top CFRP layer has a low influence and could be thin to decrease the mass of the structure without really impacting the curvature. Lastly, the top honeycomb has very little influence, meaning that the focal distance of

the optics could be changed easily without causing further bending issues. It will be fixed to 3 mm to represent the current design.

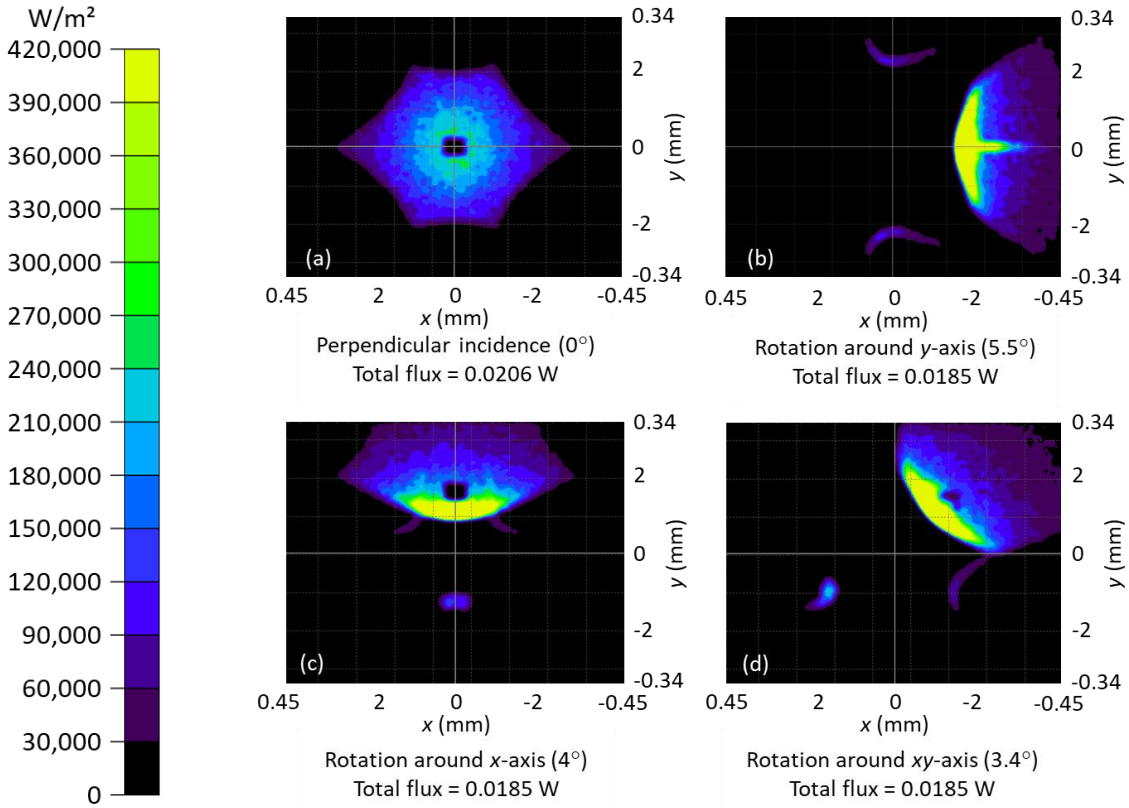

FIGURE 4. Irradiance map for a detector placed at z = - 0.15 mm from the focal point, using an integrated parabola.

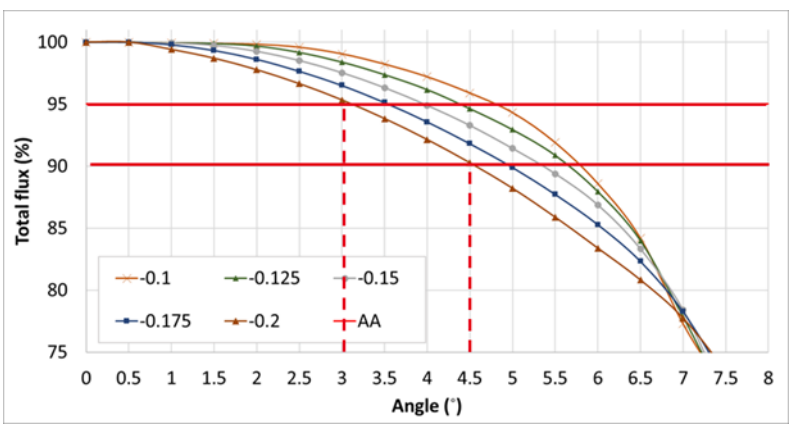

FIGURE 5. Total flux as function of the incident angle corresponding to a rotation around the y-axis.

Combining the data from the FEM and ray tracing simulations, two first configurations (A and B) were singled out, following the statistical analysis guidelines. Two other configurations (C and D) were identified by decreasing the bottom honeycomb thickness to 15 mm so as to decrease the concentrator volume by more than 50% compared to A and B. Finally, for a given configuration, it is possible to determine the maximum length of the panel for which the optical losses remain below a target. This is done by fitting the corresponding curve as explained earlier and

extrapolating to any length. In Table 3, the four selected configurations are summarized and the maximum longitudinal dimension of the panel to avoid more than a 5% optical loss is given.

TABLE 3. Comparison of the three most interesting configurations

Configuration	t_g (mm)	t_{ft} (mm)	t_{fb} (mm)	H (mm)	h (mm)	Maximum longitudinal dimension (m)
A	0.1	0.2	0.8	30	3	2.6
B	0.3	0.2	0.8	30	3	1.7
C	0.1	0.2	0.8	15	3	5.5
D	0.3	0.2	0.8	15	3	3.4

CONCLUSIONS AND PERSPECTIVES

To conclude, a parametric study on the effects of the thickness of the layers of the structure was conducted, assisted by proper design of experiments and statistical analysis. Ray tracing simulations were used to determine the optical losses associated to a modification of the incident angle. FEM simulations were performed to determine the curvature of the panel. Over whole, a method to assess the optical losses caused by the thermally induced deflection of the structure was proposed and design guidelines to minimise those losses were determined. The method is also useful to determine the maximum dimensions of a panel to avoid significant optical losses. In further studies, we will keep working on configuration D as it has the advantages of a lower volume compared to A and B (about 50%) and lower manufacturing constrains with the 300 µm thick glass compared to the 100 µm one. The thick bottom CFRP layer (0.8 mm) helps decreasing the incident angle and the top CFRP layer is thin (0.2 mm) to reduce the mass compared to a thicker one. The top honeycomb thickness is fixed at 3 mm to keep a low volume. For further work, the mechanical stress induced by the temperature changes should be investigated. The fixation of the panel as well as the thermal loading could be described more precisely in the model.

ACKNOWLEDGMENTS

This work was supported by Institut Carnot Energies du Futur.

REFERENCES

1. A. Bermudez-Garcia, P. Voarino, O. Raccurt, “Environments, needs and opportunities for future space photovoltaic power generation: A review”, *Applied Energy*, vol. 290, 2021.
2. D. M. Murphy and D. M. Allen, "SCARLET development, fabrication, and testing for the Deep Space 1 spacecraft," *IECEC-97 Proceedings of the Thirty-Second Intersociety Energy Conversion Engineering Conference (Cat. No.97CH6203)*, 1997, pp. 2237-2245 vol.4.
3. C. J. Ruud, J. S. Price, B. Fisher, B. Wang and N. C. Giebink, "Lightweight Monolithic Microcell CPV for Space," *2018 IEEE 7th World Conference on Photovoltaic Energy Conversion (WCPEC) (A Joint Conference of 45th IEEE PVSC, 28th PVSEC & 34th EU PVSEC)*, 2018, pp. 3535-3538
4. A. Bermudez-Garcia, P. Voarino, O. Raccurt, Patent No. FR2013856 (21 December 2020).
5. C.E. Kennedy, R.V. Smilgys, D.A. Kirkpatrick, J.S. Ross, “Optical performance and durability of solar reflectors protected by an alumina coating”, *Thin Solid Films*, vol. 304, p. 303-309, 1997.
6. M.J. DiGrazia and G.J. Jorgensen, “ReflecTech Mirror Film: Design Flexibility and Durability in Reflecting Solar Applications”, *American Solar Energy Society*, 2010
7. H. Torun, H. Urey, “Thermal deflections in multilayer microstructures and athermalization”, *Journal of Applied Physics*, vol. 100, n° 2, p. 023527, 2006.
8. C.H. Hsueh, “Modeling of elastic deformation of multilayers due to residual stresses and external bending”, *J. Appl. Phys*., vol. 91, n° 12, p. 9652, 2002.
9. R. R. Johnson, M. H. Kural, and G. B. Macke, “Thermal Expansion Properties of Composites Materials”, NASA Contractor Report 165632, 1981.
10. Y. Nawab, F. Jacquemin, P. Casari, N. Boyard, Y. Borjon-Piron, and V. Sobotka, *Composites Part B: Engineering*, vol. 50, p. 144-149, (2013).
11. J. Li et S. Yan, Applied Thermal Engineering, vol. 71, no 1, p. 419-432, (2014)